

A Fairness-Aware Strategy for B5G Physical-layer Security Leveraging Reconfigurable Intelligent Surfaces

A. Pierron¹, M. Barbeau², L. De Cicco³, J. Rubio-Hernan¹, J. Garcia-Alfaro¹

¹ SAMOVAR, Télécom SudParis, Institut Polytechnique de Paris, Palaiseau, France

² Carleton University, School of Computer Science, Ottawa, Canada

³ Politecnico di Bari, Dipartimento di Ingegneria Elettrica e dell'Informazione, Italy

Abstract. Reconfigurable Intelligent Surfaces are composed of physical elements that can dynamically alter electromagnetic wave properties to enhance beamforming and lead to improvements in areas with low coverage properties. When combined with Reinforcement Learning techniques, they have the potential to enhance both system behavior and physical-layer security hardening. In addition to security improvements, it is crucial to consider the concept of *fair communication*. Reconfigurable Intelligent Surfaces must ensure that User Equipment units receive their signals with adequate strength, without other units being deprived of service due to insufficient power. In this paper, we address such a problem. We explore the fairness properties of previous work and propose a novel method that aims at obtaining both an efficient and fair duplex Reconfigurable Intelligent Surface-Reinforcement Learning system for multiple legitimate User Equipment units without reducing the level of achieved physical-layer security hardening. In terms of contributions, we uncover a fairness imbalance of a previous physical-layer security hardening solution, validate our findings and report experimental work via simulation results. We also provide an alternative reward strategy to solve the uncovered problems and release both code and datasets to foster further research in the topics of this paper.

Keywords: B5G, Reconfigurable Intelligent Surface, Physical-layer Security, Fairness, User Equipment, Eavesdropping, Machine Learning, Reinforcement Learning, Deep Reinforcement Learning.

1 Introduction

The transition toward Beyond-Fifth-Generation (B5G) and 6G networks introduces challenges with respect to performance, security, and scalability [25, 36, 10]. As wireless infrastructures become increasingly heterogeneous and densely deployed, achieving reliable communication with stringent energy-efficiency requirements has become a central concern. Within this context, Reconfigurable

Intelligent Surfaces (RISs) are a recently proposed technology that allows reconfiguring the propagation environment through real-time control of electromagnetic waves [12, 11, 24, 15].

Unlike conventional architectures, RIS comprise arrays of programmable sub-wavelength elements whose reflection properties can be dynamically adjusted. This capability enables sophisticated beamforming and channel manipulation strategies that can significantly enhance network capacity and resilience [4, 30]. Potential applications span a broad range, including coverage extension in complex urban scenarios [12], energy-efficiency improvements via optimized propagation paths [20], and reinforcement of physical-layer security mechanisms [14].

The latter aspect is particularly critical. Traditional cryptographic methods operating at higher protocol layers are insufficient against vulnerabilities inherent to the physical layer. For instance, unprotected key-exchange procedures remain susceptible to replay or injection attacks, which may subsequently undermine higher-layer protections. Physical-layer security, enabled by RIS, offers a compelling approach to mitigate such threats by shaping the wireless environment itself to secure initial exchanges [14].

Despite their advantages, the integration of RISs into practical systems entails substantial challenges. Effective deployment requires taking into account unit mobility, channel variability, and real-time adaptability. These constraints are exacerbated by the limited computational and energy resources available to RIS, which are typically realized as low-power embedded devices. Moreover, in multi-user or multi-unit scenarios, fairness refers to the equitable allocation of resources, performance gains, or quality of service across participating entities. Ensuring such fairness while maintaining overall system performance introduces a complex, multi-objective optimization problem.

To address these challenges, we advocate the use of Deep Reinforcement Learning (DRL). Unlike traditional model-driven optimization methods, DRL is well suited for highly dynamic, non-linear environments, as it enables the autonomous learning of control policies through direct interaction with the system [2, 37, 35]. In particular, our approach incorporates fairness-aware mechanisms to ensure that unit-specific Quality of Service (QoS) is preserved without compromising aggregate performance or security.

The key contributions of this work are summarized as follows: (i) we uncover a fairness limitation in related work using RL-assisted physical-layer RISs security hardening, (ii) we propose a new reward strategy that tackles the problem, (iii) we validate our claims, both formally and practically; and (iv) we conclude that the new strategy can provide an equivalent level of security hardening without renouncing fairness properties.

The remaining sections are organized as follows. Section 2 reviews related literature. Section 3 formulates the problem and outlines modeling assumptions. Section 4 details the proposed methodology. Section 5 presents the evaluation results. Section 6 provides some perspectives and future directions for research. Section 7 concludes the paper and provides future work perspectives.

2 Background and Related Work

2.1 Reconfigurable Intelligent Surfaces

Reconfigurable Intelligent Surface (RIS) constitutes a novel class of engineered planar structures designed to manipulate electromagnetic (EM) waves in a nearly-passive manner [8, 12, 4]. Unlike conventional active antenna arrays, which radiate signals by means of dedicated radio-frequency (RF) chains, a RIS is composed of a large number of low-cost, sub-wavelength scattering elements, often referred to as meta-atoms or unit cells, that can locally control the phase (and, in some implementations, the amplitude) of incident EM waves. Through external control signals, these elements impose programmable reflection coefficients, thereby reshaping the propagation environment.

We consider a RIS with N reflecting elements. The baseband equivalent of the reflection matrix can be written as

$$\Theta = \text{diag}(\xi_1 e^{j\theta_1}, \xi_2 e^{j\theta_2}, \dots, \xi_N e^{j\theta_N}), \quad (1)$$

where $\theta_n \in [0, 2\pi)$ denotes the programmable phase shift of the n -th element. Assuming negligible reflection loss, each coefficient has unit modulus, i.e., $|\xi_n| = 1 \forall n \in \{1, \dots, N\}$. By jointly tuning these parameters, the RIS can reinforce constructive interference at an intended receiver or enforce destructive interference toward unintended ones.

The fundamental mechanism enabling these gains is the coherent superposition of multiple reflected signals. When the phase shifts $\{\theta_n\}$ are optimized to align with the direct and scattered channels, the received signal components add constructively, boosting the effective channel gain. Conversely, when $\{\theta_n\}$ are chosen to introduce specific phase mismatches, the scattered signals can cancel out undesired components, thus reducing interference levels or even creating nulls in certain spatial directions [38, 9]. This dual ability makes RISs attractive for interference-limited scenarios, such as dense urban deployments and cell-edge communication.

From a physical standpoint, the array gain offered by a RIS scales approximately quadratically with N under favorable propagation conditions, provided that phase coherence is maintained across all elements [8]. This property allows large surfaces to partially compensate for the so-called “double path-loss” effect caused by the cascaded transmitter–RIS–receiver channel. At the same time, the destructive interference capability provides a tool for improving spatial reuse, mitigating inter-cell interference, and enhancing physical-layer security [27, 13].

The technology underpinning RIS draws heavily from metamaterials and frequency-selective surfaces, which have long been studied in applied electromagnetics [24]. In contrast to fully active relays, which require power-hungry RF chains, RISs typically consume power only for the control circuitry, making them an energy-efficient solution for future wireless networks.

2.2 Deep Reinforcement Learning

The dynamic and complex nature of wireless networks with RIS requires advanced control strategies capable of real-time adaptation. In this context, DRL is a particularly suitable methodology, extending classical reinforcement learning methods to handle high-dimensional state and action spaces typical of such environments.

Reinforcement Learning (RL) is rooted in the principles of optimal control and dynamic programming. Early work by Bellman on dynamic programming [5] and Kalman on optimal control [22] laid the foundation for modern RL. In RL, an agent interacts with an environment, typically formalized as a Markov Decision Process (MDP) [33], to maximize the cumulative reward. At each time step t , the agent observes the system state s_t , takes an action a_t , and receives a reward r_t as the system transitions to a new state s_{t+1} . The agent's objective is to maximize the expected discounted return, expressed through the state-action value function:

$$Q^\pi(s, a) = \mathbb{E} \left[\sum_{t=0}^{\infty} \gamma^t r_t \mid s_0 = s, a_0 = a, a_t \sim \pi(s_t) \right],$$

where π is the policy mapping states to actions, and γ is the discount factor.

RL methods can be categorized along two key dimensions: *on-policy* vs *off-policy* and *value-based* vs *policy-based*. On-policy methods learn from data generated by the current policy, while off-policy methods can learn from data generated by different policies. Value-based methods focus on estimating the value function, from which a policy is derived, while policy-based methods directly optimize the policy.

The advent of deep neural networks [34, 17] gave rise to DRL, enabling RL to scale to complex, high-dimensional problems. Deep Q-Networks (DQN) is an off-policy, value-based method that uses a deep neural network to approximate the Q-function, achieving human-level performance in discrete action spaces [26].

For continuous action spaces, such as those encountered in RIS control, Deep Deterministic Policy Gradient (DDPG) [23] is particularly relevant. DDPG is an off-policy, policy-based method that combines deterministic policy gradients with an actor-critic framework. It uses a deep neural network for the actor (policy) and another for the critic (value function), with Experience Replay to improve sample efficiency [1]. This makes DDPG well-suited for the continuous control requirements of RIS-assisted communication systems.

2.3 Related Work

The intersection of DRL and RIS-assisted communication has gained considerable research attention in recent years. Liu et al. [24] provide a broad survey of the field, highlighting the adaptability of DRL-based methods to dynamic environments and their ability to optimize multiple performance objectives simultaneously.

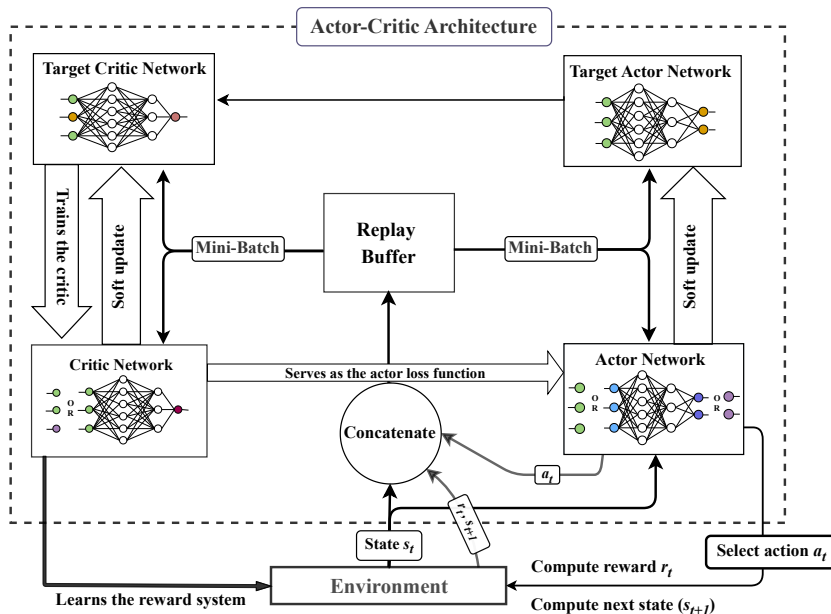


Fig. 1: General Actor–Critic architecture employed in DDPG.

Several works demonstrate the effectiveness of DRL in enhancing system performance. Nguyen et al. [29] showed that DRL-optimized RIS configurations can achieve notable gains in energy efficiency when compared to traditional non-learning, model-based schemes. Huang et al. [19] propose a DRL-driven framework for maximizing data rates while mitigating interference, while Peng et al. [32] extend this approach to duplex communication, addressing both uplink and downlink transmissions under eavesdropping threats. Similarly, Yang et al. [40] incorporate quality-of-service constraints into DRL-based optimization, underscoring the flexibility of the approach.

Despite these advances, several critical gaps remain. First, most existing studies rely on simplified channel models that do not fully capture the propagation characteristics of large-scale RIS [8]. Second, fairness in multi-unit scenarios has been largely overlooked, with optimization efforts focused primarily on aggregate system metrics. Finally, systematic comparisons across different DRL algorithms for RIS optimization remain limited, leaving open questions regarding algorithm suitability for distinct communication objectives.

3 System Considered and Problem Statement

In this section, we define the considered system and clarify the problem we want to study. Table 1 summarizes the main acronyms and notations used in our work. We consider a scenario where a Base Station (BS) with N_t transmit antennas and

Table 1: Acronyms and Notation

Acronym	Description
BS	Base Station
DRL	Deep Reinforcement Learning
UE	User Equipment
SINR	Signal-to-Noise-plus-Interference Ratio
RIS	Reconfigurable Intelligent Surface
Notation	
N	Total number of elements in the RIS
k	Number of User Equipment (UE) units
l	Number of eavesdroppers
D_i	Downlink information rate for UE $_i$
U_i	Uplink information rate of UE $_i$
R_i	Secrecy rate for unit i
$E_{i,j}$	Information rate of eavesdropper j over unit i
C	Sum secrecy rate
R_{QoS}	Quality-of-Service Reward
R_{fm}	Fairness Minimax Reward
R_{fs}	Fairness Smoothed Reward

N_r receiving antennas communicates with k legitimate UE units, each modeled as a single-antenna transceiver. A direct Line-of-Sight (LoS) link between the BS and the UEs is assumed to be blocked by an obstacle. To overcome this limitation, a RIS composed of N reflecting elements is deployed to assist both downlink and uplink communications. For tractability, we assume the network topology lies in a planar configuration [20, 19, 32].

3.1 Physical-layer Model

We build upon the general RIS-DRL setup proposed by Peng *et al.* [32] (cf. Figure 2). The system includes both legitimate UE and potential eavesdroppers, all of which are fixed in location throughout the duration of an episode. We retain the propagation model, interference treatment, and Signal-to-Noise-plus-Interference Ratio (SINR) computation used in [32], while adapting the channel modeling to better capture the physical behavior of RIS, as detailed in [8].

Both the BS and RIS are modeled as Uniform Linear Arrays (ULAs). The LoS channel components follow the physically consistent formulation in [8], and we do not consider the Non Line-of-Sight (NLoS) components of the signal for simplification.

We compute the array response channel \mathbf{H}_t^r between a transmitter \mathbf{t} and receiver \mathbf{r} as

$$\mathbf{H}_t^r = \begin{bmatrix} 1 \\ \vdots \\ e^{-j2\pi \frac{(A_r-1)\Delta \sin \varphi_r}{\lambda}} \end{bmatrix} \begin{bmatrix} 1 \dots e^{-j2\pi \frac{(A_t-1)\Delta \sin \varphi_t}{\lambda}} \end{bmatrix}, \quad (2)$$

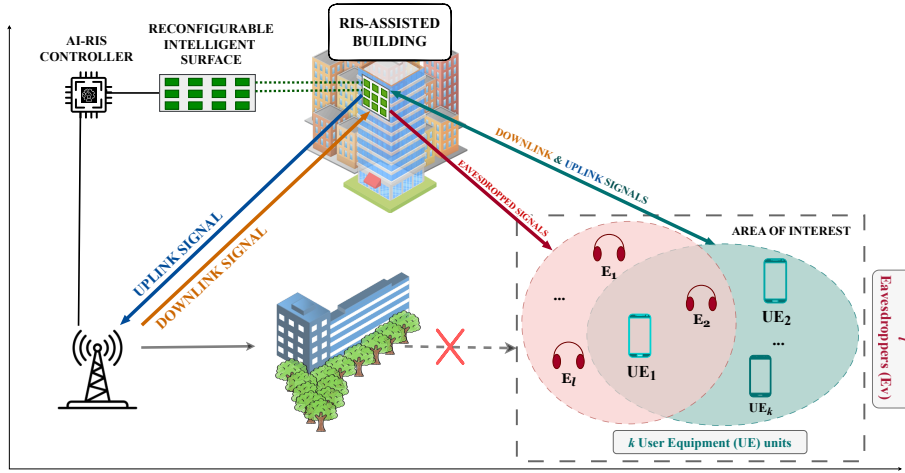


Fig. 2: Considered RIS-DRL environment with multiple UEs and eavesdroppers.

where λ is the wavelength, φ_t and φ_r denote the Angle-of-Departure (AoD) and Angle-of-Arrival (AoA), respectively, Δ is the antenna spacing, and A_t and A_r are the number of antennas at transmitter and receiver.

The large-scale channel gain β for the BS–RIS–UE cascade is derived from [8]:

$$\beta_t = \frac{G_t(\phi_t, \theta_t) A_m}{4\pi d_t^2}, \quad \beta_r = \frac{G_r(\phi_r, \theta_r) A_m}{4\pi d_r^2}, \quad (3)$$

$$\beta = N^2 \beta_t \beta_r = N^2 \frac{G_t(\phi_t, \theta_t) G_r(\phi_r, \theta_r) A_m^2}{(4\pi d_t d_r)^2}, \quad (4)$$

where d_t and d_r denote the distances from transmitter and receiver to the RIS, respectively, A_m is the area of each reflecting element (approximated as $(\lambda/4)^2$), and G_t, G_r are respectively the antenna gain functions at the transmitter and the receiver, with ϕ_t, ϕ_r azimuth angles and θ_t, θ_r elevation angles. As shown in [8], the RIS gain scales quadratically with N , making very large surfaces suitable to offset the cascaded path losses. Throughout this work, we assume the RIS is a Uniform Linear Array (ULA) constituted of isotropic antennas with a normalized gain, $G_t = G_r = 1$. This assumption simplifies our analysis by focusing on the inherent properties of the RIS and use cases of mobile communications such as B5G networks [3, 8].

3.2 Threat Model

We consider eavesdroppers as the primary adversaries in the system, representing the main physical-layer threat to RIS-assisted communication. Eavesdroppers aim to intercept downlink or uplink transmissions whenever they fall within the high-gain region of the beam. Following Peng et al. [32], Yang et al. [40], we

assume l eavesdroppers attempting to capture the transmitted signals. Although this model is simplified, it effectively captures a realistic security concern, as RIS beamforming can inadvertently create unintended high-gain lobes toward external nodes. These lobes can expose sensitive transmissions to interception by unauthorized receivers. Therefore, secrecy analysis is essential to ensure robust and confidential communication in RIS-assisted systems.

3.3 Controller Model

Our DRL agent controls both the BS beamforming matrix $\mathbf{W} \in \mathbb{C}^{N_t \times k}$ and the RIS diagonal phase-shift matrix $\boldsymbol{\Theta} \in \mathbb{C}^{N \times N}$, whose entries are unit-modulus complex exponentials. The transmit power constraint at the BS is enforced by projecting \mathbf{W} as

$$\Pi(\mathbf{W}) = \begin{cases} \mathbf{W}, & \text{if } \text{Tr}(\mathbf{W}\mathbf{W}^H) \leq P_{\max}, \\ \frac{\sqrt{P_{\max}}}{\|\mathbf{W}\|_F} \mathbf{W}, & \text{otherwise,} \end{cases} \quad (5)$$

where $\|\cdot\|_F$ denotes the Frobenius norm.

We employ the DDPG algorithm [23] for continuous control (cf Section 2.2). The observation vector s_t at time t includes the cascaded channel state, phase noise, previous slot rates, and the action applied at $t-1$, following Peng et al. [32].

3.4 Problem Formulation

We can now formalize the optimization problem. First, we introduce common terms and the baseline reward function.

For each unit i , the achievable downlink and uplink data rates are

$$D_i = \log_2(1 + \text{SINR}_i^D), \quad (6)$$

$$U_i = \log_2(1 + \text{SINR}_i^U), \quad (7)$$

where SINR_i^D and SINR_i^U are the downlink and uplink SINRs, respectively. The data rate overheard by eavesdropper j from unit i is

$$E_{i,j} = \log_2(1 + \text{SINR}_{d,i,j}^E) + \log_2(1 + \text{SINR}_{u,i,j}^E), \quad (8)$$

where $\text{SINR}_{d,i,j}^E$ and $\text{SINR}_{u,i,j}^E$ denote the downlink and uplink SINR components as seen by the eavesdropper. These quantities form the building blocks of the secrecy-aware reward functions.

Following Peng et al. [32], the secrecy rate for unit i is

$$R_i = \left[D_i + U_i - \max_j E_{i,j} \right]^+, \quad (9)$$

where $[x]^+ = \max(0, x)$. The baseline reward, i.e., the Sum Secrecy Rate (SSR), is then defined as

$$C = \sum_{i=1}^k R_i. \quad (10)$$

This reward emphasizes overall capacity and secrecy, without fairness or QoS guarantees, and is widely adopted in the literature [19, 8]. In our experiments, we denote this reward as the *baseline*.

The overall objective is to maximize a chosen reward function under the system constraints. For the baseline SSR reward, this yields:

$$\begin{aligned} & \underset{\mathbf{W}, \boldsymbol{\Theta}}{\text{maximize}} && C(\mathbf{W}, \boldsymbol{\Theta}, \boldsymbol{\Phi}, \mathcal{H}) \\ & \text{subject to} && \text{Tr}(\mathbf{W}\mathbf{W}^H) \leq P_{\max}, \\ & && 0 \leq \theta_m < 2\pi, \quad m = 1, \dots, N. \end{aligned} \quad (11)$$

where \mathcal{H} denotes the set of all channels involved in the communication scenario. Alternative reward formulations incorporating fairness (cf. Section 4.2) or QoS guarantees can replace C , enabling flexible control of system objectives.

3.5 Fairness Model

In addition to secrecy and capacity, fairness among units is a key performance dimension. Without fairness, strong channels or favorable spatial locations may monopolize resources, while disadvantaged units experience poor service. To quantify this, we adopt the Jain Fairness Index (JFI) [21]:

$$I_{\text{Jain}} = \frac{\left(\sum_{i=1}^k R_i\right)^2}{k \cdot \sum_{i=1}^k R_i^2}, \quad (12)$$

where R_i is the secrecy rate of unit i . The index ranges from $1/k$ to 1, with unity indicating perfect equal distribution of the rewards between each participant, meaning perfect fairness.

A fundamental trade-off, named *price of fairness*, exists between maximizing total capacity and ensuring fairness [7]. As highlighted in [8], optimizing purely for sum rate often leads to uneven allocations, since resources are concentrated on units with favorable channels. Conversely, enforcing strict fairness (e.g., maximizing the minimum secrecy rate) generally lowers the aggregate capacity.

This trade-off is of practical importance in B5G-6G scenarios where both high throughput and equitable unit experience are essential. For example, ultra-reliable low-latency communication services may prioritize fairness, while enhanced mobile broadband services lean toward capacity maximization. Our study explicitly integrates this trade-off into the reward functions explored in Section 4, thereby enabling control over system-wide fairness levels.

4 Reward Functions and Fairness Improvements

The objective of this section is to address the fairness issues discussed in Section 2.3. We also design a new reward strategy that maximizes the legitimate data rate transmitted to UE, while maintaining the same level of security enhancement. We seek to ensure that each unit receives a minimum usable data rate. The goal is to provide a fair service among all units despite the non-linearity of our optimization problem. Next, we explore further the reward functions selected for our work.

4.1 Quality-of-Service-Aware Reward Function

The reward function in Yang et al. [40] introduces unit-specific Quality-of-Service (QoS) constraints. The reward, denoted here as the *QoS* reward, is given by

$$R_{QoS} = \sum_{i=1}^k (R_i - \mu_1 p_i^S - \mu_2 p_i^U), \quad (13)$$

where μ_1 and μ_2 are positive constants balancing penalties for matching respectively the security and transmission criteria, and

$$p_i^S = \begin{cases} 1, & \text{if } R_i < \epsilon_i^S, \\ 0, & \text{otherwise} \end{cases}$$

$$p_i^U = \begin{cases} 1, & \text{if } D_i + U_i < \epsilon_i^U, \\ 0, & \text{otherwise} \end{cases}$$

with $\epsilon_i^S, \epsilon_i^U \in \mathbb{R}^+$ denoting respectively the target secrecy rate for the i -th UE and the target data rate.

This formulation introduces a first notion of service by penalizing configurations where individual units fail to meet their minimum requirements. However, once thresholds are satisfied, the system remains free to allocate resources disproportionately, favoring specific units to maximize overall reward. This limitation motivates the need for fairness-aware extensions.

4.2 Fairness-aware Reward Function

As discussed in Section 3.5, balancing overall system capacity and security with fairness among units represents a critical tradeoff in RIS-assisted communication. The baseline reward function provides no explicit incentive to distribute resources equitably, while the *QoS* reward in (13) ensures only a minimum rate per unit without addressing fairness beyond threshold satisfaction. To overcome these limitations, we introduce fairness-aware reward formulations that explicitly account for equitable resource distribution in both downlink and uplink.

We define the following intermediate terms for unit i :

$$\begin{aligned}
R_{di} &= \left[D_i - \max_{j \in [1:l]} \log_2 (1 + \text{SINR}_{d,i,j}^E) \right]^+, \\
R_{ui} &= \left[U_i - \max_{j \in [1:l]} \log_2 (1 + \text{SINR}_{u,i,j}^E) \right]^+, \\
R_d &= \min_{i \in [1:k]} R_{di}, \\
R_u &= \min_{i \in [1:k]} R_{ui},
\end{aligned}$$

By construction, R_d and R_u represent the bottleneck unit rates in each direction, thereby embedding fairness into the optimization process. Based on these terms, we propose two candidate reward functions:

$$R_{fm} = k \cdot (R_d + R_u), \quad (14)$$

$$R_{fs} = \left(\frac{\sum_{i=1}^k R_{di}}{1 + \text{std}(R_{di})} \right)^{p_f} + \left(\frac{\sum_{i=1}^k R_{ui}}{1 + \text{std}(R_{ui})} \right)^{p_f}, \quad (15)$$

where R_{fm} emphasizes the minimum guaranteed rate across units by using a minimax approach [8], R_{fs} penalizes large rate disparities by incorporating the standard deviation of per-unit performance and $p_f \in \mathbb{N}$ is a hyperparameter.

Equation (14) implements a hard minimax objective by depending only on the bottleneck rates $\min_i R_{di}$ and $\min_i R_{ui}$. Although this gives strict worst-case guarantees, the nested max, min and the $[\cdot]^+$ operator produce a highly non-smooth, piecewise reward surface. In RIS-assisted beamforming, small changes in phase shifts or power allocations can abruptly change which unit is worst-off, causing discontinuous jumps in R_{fm} . Such discontinuities and the underlying non-convexity significantly impair gradient-based or sample-limited RL algorithms, as they increase gradient variance, induce slow or unstable convergence, and make the policy highly sensitive to initialization. Moreover, a pure minimax objective is inherently conservative: raising the minimum often forces large sacrifices in aggregate throughput.

By contrast, Equation (15) acts as a smooth surrogate that explicitly trades off aggregate throughput and dispersion. The numerator rewards overall secrecy performance while the denominator penalizes unequal allocations; the additive constant prevents numerical instability when the spread is small. This ratio (i) yields a denser, more informative learning signal because every unit contributes to the reward (unlike the minimum which depends only on the single worst unit), (ii) produces a smoother optimization landscape that reduces gradient variance and improves training stability in the high-dimensional, nonconvex RIS action space, and (iii) allows the designer to tune the fairness/throughput trade-off via the exponent p_f . For these reasons R_{fs} is a practically relevant, trainable

compromise when using learning-based controllers, whereas R_{fm} remains appropriate if one requires strict, provable guarantees on the worst-case unit.

We name these two reward functions respectively the fm and fs rewards for *fairness minimax* and *fairness smoothed*.

5 Experimental Framework and Results

In this section, we present the experimental framework and simulation results. We first describe the design of the framework and the adopted algorithms, and then analyze the system performance in terms of capacity, fairness, and robustness against eavesdroppers. To ensure reproducibility, the full code is publicly released in a companion repository.[§]

5.1 Framework Features

The proposed framework provides a DRL environment tailored for duplex communications between a BS and multiple UE units, assisted by a RIS. The environment is implemented in Python, with all DRL algorithms developed using PyTorch. The framework is openly available to reproduce our experiments and to support further research on the application of DRL to RIS-aided communication systems.

The system includes monitoring tools to evaluate learning dynamics and performance metrics, thereby providing a complete overview of the training process. In this study, we adopt the DDPG algorithm [23], following the actor-critic architecture previously used in [32, 19]. Both the actor and the critic use a Multi-Layer Perceptron (MLP) [18]. The state space is unchanged from Peng *et al.* [32], while the algorithm itself follows its original implementation [23, 16], except for modifications to the reward functions in order to reflect the objectives defined in Section 4.

5.2 Experimental Setup

We consider three representative scenarios: one without eavesdroppers and two with eavesdroppers. The environment remains consistent in all scenarios. The BS, positioned at coordinates $(0, 0)$, communicates with the RIS located at $(20, 100)$ in both directions. Each scenario is trained over 40 000 steps. The BS is equipped with $N_t = N_r = 4$ antennas, while the RIS consists of $N = 36$ elements. We consider two legitimate UE units, *i.e.*, $k = 2$. In the scenarios with eavesdroppers, we assume l is also set to two eavesdroppers. We use a wavelength $\lambda = 0.1$ m, a maximum emitting power of 20 dBm for the BS and 100 mW for the legitimate units.

Scenario 1 corresponds to a baseline case without eavesdroppers, used to illustrate the trade-off between capacity and fairness in the absence of external

[§]https://github.com/alex-pierron/CTRL_RIS

Table 2: Main hyperparameters used

Parameter	Value
Actor learning rate (δ_a)	1×10^{-5}
Critic learning rate (δ_c)	1×10^{-3}
Soft update coefficient (τ)	5×10^{-4}
Replay buffer size	5000
Batch size	96
Actor update frequency	Every two steps
Critic update frequency	Every step
Training steps	40 000
Target Data Rate ϵ_i^U	2.5
Target Secrecy Rate ϵ_i^S	1.5
μ_1	2
μ_2	2
p_f	2

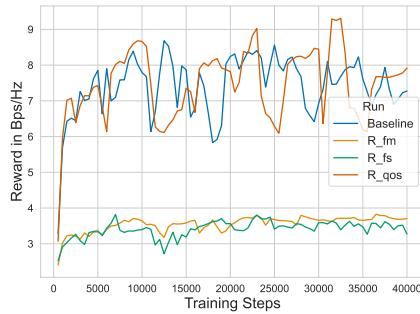
threats. Scenario 2 introduces eavesdroppers positioned close to the legitimate users: the UE units are placed at (147, 20) and (169, 80), while the eavesdroppers are placed at (140, 40) and (150, 75). Scenario 3 considers a different spatial arrangement, where the legitimate units are at (124, 40) and (138.5, 81) and the eavesdroppers at (132, 50) and (128, 85).

Each scenario is trained with a dedicated controller, since DRL methods are highly sensitive to hyperparameter tuning. The training and neural network main settings are summarized in Table 2 and also include the main hyperparameters for the reward functions. The full detailed hyperparameter value list is also available at our public GitHub repository.

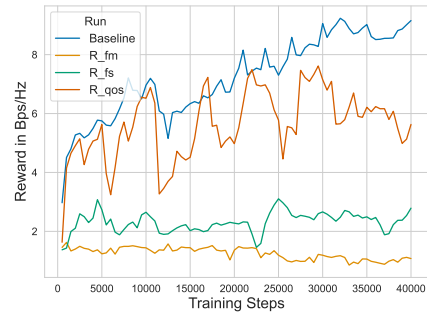
5.3 Results

The performance of the different reward functions introduced in Section 4 is evaluated in terms of capacity, fairness, and robustness against eavesdroppers. All metrics are normalized with respect to the *baseline* reward function to enable consistent comparisons.

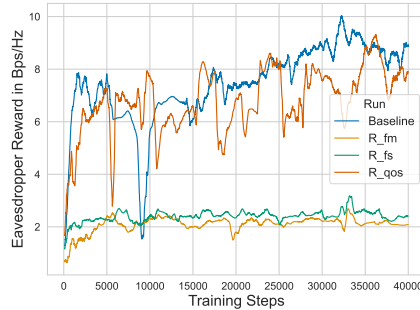
The evolution of system capacity is shown in Figure 3, while Figure 4 reports the fairness measured using the Jain Fairness Index (JFI). In Scenario 1, the *baseline* and *QoS* rewards achieve higher capacity, almost twice as high on average as that obtained with the *fm* and *fs* rewards. However, this gain comes at the expense of fairness: the average JFI is around 0.5, which corresponds to a completely unfair allocation. By contrast, the *fm* and *fs* rewards lead to substantially higher fairness, with an average JFI close to 0.9, though at the cost of reduced capacity. Notice that this result is expected and confirms the generality of the *price of fairness* property described in Section 3.5, *i.e.*, the price to pay to make the allocation fair [7].



(a) Scenario 1



(b) Scenario 2



(c) Scenario 3

Fig. 3: Evolution of system capacity with respect to the *baseline* reward in Scenarios 1–3. Each plot represents the baseline reward over time (local average) in Bps/Hz. Results are smoothed with a rolling window of size 500.

The same trade-off is observed in Scenarios 2 and 3, which involve eavesdroppers. While reaching high fairness becomes more difficult, the *fm* and *fs* functions still achieve a significantly better balance compared to the baseline and QoS functions, confirming the robustness of their fairness-oriented design.

The analysis of eavesdropper performance, shown in Figure 5, provides further insights. When using the *baseline* reward, the eavesdroppers benefit from improved performance in parallel with the legitimate users. Conversely, with *fm* and *fs*, the rewards obtained by the eavesdroppers remain consistently lower, indicating that these reward functions also provide improved security by limiting information leakage.

The *fm* and *fs* reward functions enhance fairness and robustness against eavesdroppers, but at the cost of raw system capacity. This trade-off highlights the importance of carefully designing reward mechanisms to meet system-level objectives. The experimental evaluation demonstrates that fairness-aware reward formulations can effectively balance the competing demands of system capacity,

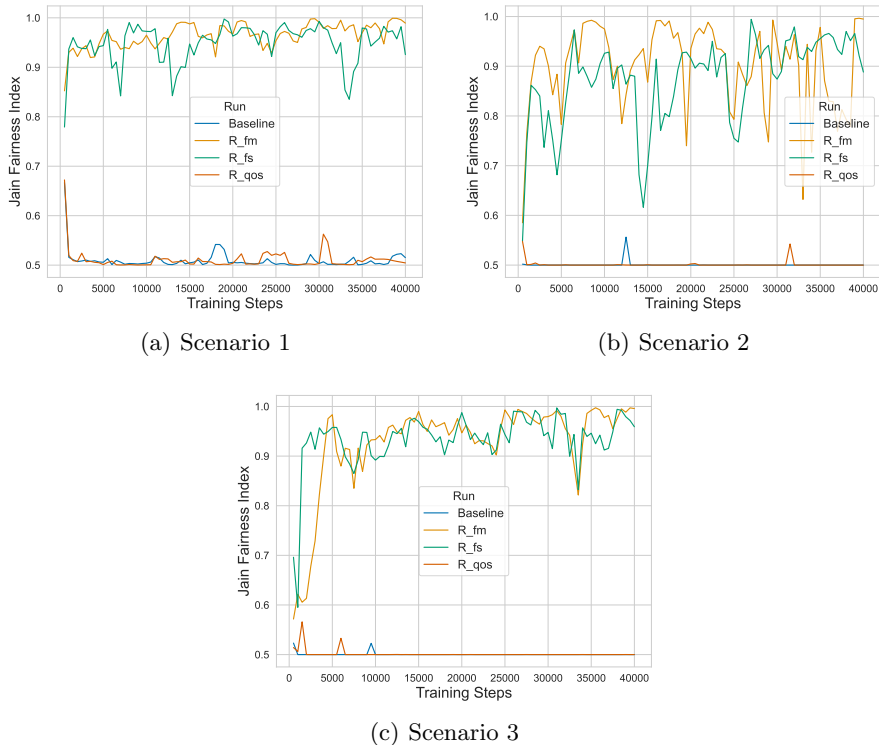


Fig. 4: Evolution of Jain Fairness Index (JFI) in Scenarios 1–3. Each plot represents user JFI over time (local average). Results are smoothed with a rolling window of size 500.

equitable resource allocation, and physical-layer security, providing valuable insights for the design of practical RIS-assisted communication systems.

Additional experimental data, detailed plots, and TensorBoard logs are available in the companion repository¹ to facilitate further analysis and reproducibility.

6 Future Directions for Research

Several promising research directions emerge from this work. First, the development of general controllers capable of operating in diverse environment configurations represents a significant challenge. Current DRL methods require careful hyperparameter tuning and are highly sensitive in order to properly generalize. Training a single controller that can adapt to varying network topologies,

¹https://github.com/alex-pierron/CTRL_RIS

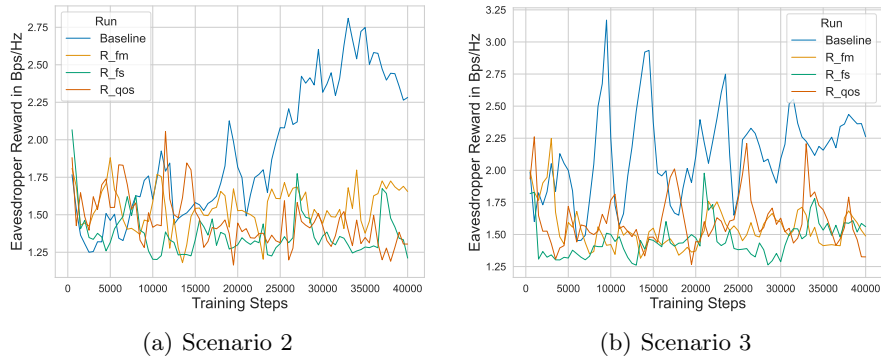


Fig. 5: Eavesdroppers’ rewards with respect to the *baseline* reward in Scenarios 2 and 3. Each plot represents the eavesdropper reward over time (local average) in Bps/Hz. Results are smoothed with a rolling window of size 500.

user distributions, and threat models would substantially improve the practical applicability of DRL-based RIS control. This generalization problem could be addressed through curriculum learning [6, 28], imitation learning [41] or transfer learning techniques [31, 42] that leverage knowledge from previously trained controllers. Since DRL controllers would ultimately be embedded on the RIS, their inference performance should be systematically compared with non-learning, model-based optimization methods to assess practical deployment trade-offs.

Second, a systematic comparison with non-learning, model-based optimization baselines would provide valuable insights into the trade-offs between DRL approaches and traditional optimization methods. While DRL offers adaptability to dynamic environments, model-based techniques such as semidefinite programming or alternating optimization may provide more interpretable solutions and computational guarantees. Understanding when each approach is preferable would help guide practical system design.

Third, the RIS model could be refined to better capture practical hardware constraints. Decoupling uplink and downlink elements would enable more realistic duplex communication modeling [24, 39], while incorporating amplitude control and accounting for quantization errors would provide more faithful representations of real-world RIS implementations.

Finally, dynamic scenarios using relevant mobility patterns for the users and eavesdroppers present an important extension. Investigating how fairness-aware reward functions perform under such dynamic conditions while maintaining fairness guarantees would be a relevant research direction.

7 Conclusion

We explored the concept of *fair communications* in DRL-enabled RIS environments. We assumed that RISs must ensure that UE units receive their signals

with adequate strength, without other UE being deprived of service due to insufficient power. We investigated this problem and examined the fairness properties of previous work. We proposed a novel method that aims at obtaining an efficient and fair duplex DRL-RIS system for multiple legitimate UE units. We reported experimental work and simulation results, and released our code and experiments to foster further research on this topic.

The results show that fairness-oriented reward functions can significantly improve the equity of resource allocation and mitigate information leakage to eavesdroppers, at the expense of raw system capacity. This trade-off illustrates the difficulty of achieving both high capacity and strong fairness in RIS-assisted systems and is consistent with general fair resource allocation theory.

It is important to acknowledge the inherent sensitivity of deep reinforcement learning to hyperparameters. Fine-tuning such algorithms requires substantial effort, as performance is highly sensitive to hyperparameter choices, network architectures, and training conditions.

In this study, we therefore restricted our experiments to subcases with dedicated controllers. Based on these limitations and the insights gained from our work, we have identified several promising future research directions, including the development of general controllers that can adapt across diverse network configurations, systematic comparisons with model-based optimization methods, refinements to capture practical RIS hardware constraints, and extensions to dynamic scenarios with user and eavesdropper mobility.

Acknowledgments. The work is supported by the French National Research Agency under the France 2030 label (NF-HiSec ANR-22-PEFT-0009).

References

- [1] Adam, S., Busoniu, L., Babuska, R.: Experience replay for real-time reinforcement learning control. *IEEE Transactions on Systems, Man, and Cybernetics, Part C (Applications and Reviews)* **42**(2), 201–212 (2011)
- [2] Arulkumaran, K., Deisenroth, M.P., Brundage, M., Bharath, A.A.: Deep reinforcement learning: A brief survey. *IEEE signal processing magazine* **34**(6), 26–38 (2017)
- [3] Balanis, C.A.: *Antenna Theory: Analysis and Design*. Wiley, 4th edn. (2016), ISBN 978-1-118-64206-1
- [4] Basar, E., Di Renzo, M., De Rosny, J., Debbah, M., Alouini, M.S., Zhang, R.: Wireless communications through reconfigurable intelligent surfaces. *IEEE access* **7**, 116753–116773 (2019)
- [5] Bellman, R.: *Dynamic Programming*. Princeton University Press, Princeton, NJ (1957)

- [6] Bengio, Y., Louradour, J., Collobert, R., Weston, J.: Curriculum learning. In: Proceedings of the 26th annual international conference on machine learning, pp. 41–48 (2009)
- [7] Bertsimas, D., Farias, V.F., Trichakis, N.: The price of fairness. *Operations Research* **59**(6), 1380–1393 (2011), <https://doi.org/10.1287/opre.1100.0865>
- [8] Björnson, E., Demir, Ö.T., et al.: Introduction to multiple antenna communications and reconfigurable surfaces. Now Publishers, Inc. (2024)
- [9] Björnson, E., Sanguinetti, L.: Power control and scheduling for cellular-connected uavs with reconfigurable intelligent surfaces. *IEEE Transactions on Wireless Communications* **20**(4), 2551–2565 (2020)
- [10] Chen, W., Lin, X., Lee, J., Toskala, A., Sun, S., Chiasserini, C.F., Liu, L.: 5g-advanced toward 6g: Past, present, and future. *IEEE journal on selected areas in communications* **41**(6), 1592–1619 (2023)
- [11] Dai, L., Wang, B., Wang, M., Yang, X., Tan, J., Bi, S., Xu, S., Yang, F., Chen, Z., Di Renzo, M., et al.: Reconfigurable intelligent surface-based wireless communications: Antenna design, prototyping, and experimental results. *IEEE access* **8**, 45913–45923 (2020)
- [12] Di Renzo, M., Zappone, A., Debbah, M., Alouini, M.S., Yuen, C., De Rosny, J., Tretyakov, S.: Smart radio environments empowered by reconfigurable intelligent surfaces: How it works, state of research, and the road ahead. *IEEE Journal on Selected Areas in Communications* **38**(11), 2450–2525 (2020)
- [13] Di Renzo, M., et al.: Smart radio environments empowered by reconfigurable intelligent surfaces: An idea whose time has come. *EURASIP Journal on Wireless Communications and Networking* **2020**(1), 129 (2020)
- [14] Do, D.T., Le, A.T., Ha, N.D.X., Dao, N.N.: Physical layer security for Internet of Things via reconfigurable intelligent surface. *Future Generation Computer Systems* **126**, 330–339 (2022)
- [15] ETSI ISG RIS: Reconfigurable Intelligent Surfaces (RIS); Use Cases, Deployment Scenarios and Requirements. Tech. Rep. V1.2.1, European Telecommunications Standards Institute (ETSI) (February 2025), URL https://www.etsi.org/deliver/etsi_gr/RIS/001_099/001/01.02.01_60/gr_RIS001v010201p.pdf
- [16] Fujimoto, S., Hoof, H., Meger, D.: Addressing function approximation error in actor-critic methods. In: International conference on machine learning, pp. 1587–1596, PMLR (2018)
- [17] Goodfellow, I., Bengio, Y., Courville, A.: Deep learning. MIT Press (2016)
- [18] Hornik, K., Stinchcombe, M., White, H.: Multilayer feedforward networks are universal approximators. *Neural Networks* **2**(5), 359–366 (1989)
- [19] Huang, C., Mo, R., Yuen, C.: Reconfigurable intelligent surface assisted multiuser MISO systems exploiting deep reinforcement learning. *IEEE Journal on Selected Areas in Communications* **38**(8), 1839–1850 (2020)
- [20] Huang, C., Zappone, A., Alexandropoulos, G.C., Debbah, M., Yuen, C.: Reconfigurable intelligent surfaces for energy efficiency in wireless communication. *IEEE transactions on wireless communications* **18**(8), 4157–4170 (2019)

- [21] Jain, R.K., Chiu, D.M.W., Hawe, W.R., et al.: A quantitative measure of fairness and discrimination. Tech. rep., Digital Equipment Corporation (1984)
- [22] Kalman, R.E.: Contributions to the theory of optimal control. *Boletín de la Sociedad Matemática Mexicana* **5**(2), 102–119 (1960)
- [23] Lillicrap, T.P., Hunt, J.J., Pritzel, A., Heess, N., Erez, T., Tassa, Y., Silver, D., Wierstra, D.: Continuous control with deep reinforcement learning. In: *Proceedings of the 33rd International Conference on Machine Learning* (2016)
- [24] Liu, Y., Liu, X., Mu, X., Hou, T., Xu, J., Di Renzo, M., Al-Dhahir, N.: Reconfigurable Intelligent Surfaces: Principles and Opportunities. *IEEE Communications Surveys & Tutorials* **23**(3), 1546–1577 (2021)
- [25] Mao, B., Liu, J., Wu, Y., Kato, N.: Security and privacy on 6g network edge: A survey. *IEEE communications surveys & tutorials* **25**(2), 1095–1127 (2023)
- [26] Mnih, V., Kavukcuoglu, K., Silver, D., Rusu, A.A., Veness, J., Belle-mare, M.G., Graves, A., Riedmiller, M., Fidjeland, A.K., Ostrovski, G., et al.: Human-level control through deep reinforcement learning. *Nature* **518**(7540), 529–533 (2015)
- [27] Najafi, M., Schober, R., Poor, H.V.: Physics-based modeling and scalable optimization of large intelligent reflecting surfaces. *IEEE Transactions on Wireless Communications* **20**(8), 5514–5530 (2021)
- [28] Narvekar, S., Peng, B., Leonetti, M., Sinapov, J., Taylor, M.E., Stone, P.: Curriculum learning for reinforcement learning domains: A framework and survey. *Journal of Machine Learning Research* **21**(181), 1–50 (2020)
- [29] Nguyen, T.V., Truong, T.P., Nguyen, T.M.T., Noh, W., Cho, S.: Achievable rate analysis of two-hop interference channel with coordinated IRS relay. *IEEE Transactions on Wireless Communications* **21**(9), 7055–7071 (2022)
- [30] Pan, C., Zhou, G., Zhi, K., Hong, S., Wu, T., Pan, Y., Ren, H., Di Renzo, M., Swindlehurst, A.L., Zhang, R., et al.: An overview of signal processing techniques for ris/irs-aided wireless systems. *IEEE Journal of Selected Topics in Signal Processing* **16**(5), 883–917 (2022)
- [31] Pan, S.J., Yang, Q.: A survey on transfer learning. *IEEE Transactions on knowledge and data engineering* **22**(10), 1345–1359 (2009)
- [32] Peng, Z., Zhang, Z., Kong, L., Pan, C., Li, L., Wang, J.: Deep reinforcement learning for RIS-aided multiuser full-duplex secure communications with hardware impairments. *IEEE Internet of Things Journal* **9**(21), 21121–21135 (2022)
- [33] Puterman, M.L.: *Markov Decision Processes: Discrete Stochastic Dynamic Programming*. John Wiley & Sons (2014)
- [34] Rumelhart, D.E., Hinton, G.E., Williams, R.J.: Learning representations by back-propagating errors. *Nature* **323**(6088), 533–536 (1986)
- [35] Tang, C., Abbatematteo, B., Hu, J., Chandra, R., Martín-Martín, R., Stone, P.: Deep reinforcement learning for robotics: A survey of real-world successes. In: *Proceedings of the AAAI Conference on Artificial Intelligence*, vol. 39, pp. 28694–28698 (2025)